JEM Journal of Experimental Medicine

ARTICLE

Diminished cell proliferation promotes natural killer cell adaptive-like phenotype by limiting FcεRIγ expression

Avishai Shemesh[1,2], Yapeng Su[3], Daniel R. Calabrese[4,5], Daniel Chen[3,6,7], Janice Arakawa-Hoyt[1], Kole T. Roybal[1,2,8,9,10,11], James R. Heath[3,12], John R. Greenland[4,5], and Lewis L. Lanier[1,2]

Human adaptive-like natural killer (NK) cells express low levels of FcεRIγ (FcRγ$^{-/low}$) and are reported to accumulate during COVID-19 infection; however, the mechanism underlying and regulating FcRγ expression in NK cells has yet to be fully defined. We observed lower FcRγ protein expression in NK cell subsets from lung transplant patients during rapamycin treatment, suggesting a link with reduced mTOR activity. Further, FcRγ$^{-/low}$ NK cell subsets from healthy donors displayed reduced mTOR activity. We discovered that FcRγ upregulation is dependent on cell proliferation progression mediated by IL-2, IL-15, or IL-12, is sensitive to mTOR suppression, and is inhibited by TGFβ or IFNα. Accordingly, the accumulation of adaptive-like FcRγ$^{-/low}$ NK cells in COVID-19 patients corresponded to increased TGFβ and IFNα levels and disease severity. Our results show that an adaptive-like NK cell phenotype is induced by diminished cell proliferation and has an early prognostic value for increased TGFβ and IFNα levels in COVID-19 infection associated with disease severity.

Introduction

NK cells are innate lymphocytes with adaptive features, functionally regulated by activating and inhibitory germline-encoded receptors (Cerwenka and Lanier, 2016; Sun et al., 2009; Schlums et al., 2015). The adaptor FcRγ is encoded by the *FCER1G* gene and forms homodimers or heterodimers with the adaptor CD3ζ. These adaptor dimers assemble a molecular complex with the activating receptors CD16 (*FcγRIII*), NKp30, or NKp46 on the cell surface of human NK cells (Lanier, 2009; Liu et al., 2020). Human peripheral blood immature NK cells (CD3$^-$CD56^{bright}CD16$^-$NKG2A$^+$) express low FcRγ levels, whereas mature NK cells (CD3$^-$CD56^{dim}CD16$^+$NKG2A$^\pm$) show increased FcRγ expression (Cooper et al., 2001; Björkström et al., 2010; Lopez-Vergès et al., 2010). A subset of mature NK cells designated adaptive NK cells is characterized by low or negative FcRγ expression and reduced expression of PLZF, Siglec-7, Syk, CD161, NKG2A, NKp30, and NKp46 (Schlums et al., 2015; Lee et al., 2015). CRISPR knockout of the *FCER1G* gene induces adaptive-like features in human NK cells (Liu et al., 2020). Adaptive or adaptive-like FcRγ$^{-/low}$ NK cells are found in healthy individuals' peripheral blood and solid tissues including the lung and exhibit stable long-term population frequencies (Muccio et al., 2018; Brownlie et al., 2021).

The expansion of adaptive FcRγ$^{-/low}$ NK cells is associated with human cytomegalovirus (HCMV) infection and higher expression of the activating receptor CD94-NKG2C (Schlums et al., 2015; Brownlie et al., 2021; Lee et al., 2015). However, the adaptive NK cell phenotype is not confined to NKG2C-expressing cells alone, and the stimuli driving their differentiation are unknown (Liu et al., 2016). In vivo, anti-HCMV antibody titers and HCMV UL40 peptide-induced CD94-NKG2C–dependent NK cell activation correlate with increased frequencies of adaptive NK cells in HMCV-infected individuals (Lee et al., 2015; Rölle et al., 2018; Wu et al., 2013). Ex vivo CD16 stimulation is suggested to expand adaptive FcRγ$^{-/low}$ cells relative to nonadaptive FcRγ^{high} NK cells due to the CD16 transmembrane domain interaction with CD3ζ homodimers (Schlums et al., 2015; Lee et al., 2015; Liu et al., 2020; Lanier et al., 1991). Adaptive or adaptive-like NK cells alter the risk for myeloma

[1]Department of Microbiology and Immunology, University of California, San Francisco, San Francisco, CA; [2]Parker Institute for Cancer Immunotherapy, University of California, San Francisco, San Francisco, CA; [3]Institute for Systems Biology, Seattle, WA; [4]Department of Medicine, University of California, San Francisco, CA; [5]Medical Service, Veterans Affairs Health Care System, San Francisco, CA; [6]Department of Microbiology, University of Washington, Seattle, WA; [7]Department of Informatics, University of Washington, Seattle, WA; [8]Helen Diller Family Comprehensive Cancer Center, University of California, San Francisco, San Francisco, CA; [9]Chan Zuckerberg Biohub, San Francisco, CA; [10]Gladstone University of California, San Francisco Institute for Genetic Immunology, San Francisco, CA; [11]University of California, San Francisco Cell Design Institute, San Francisco, CA; [12]Department of Bioengineering, University of Washington, Seattle, WA.

Correspondence to Avishai Shemesh: avishaish83@gmail.com; Lewis L. Lanier: lewis.lanier@ucsf.edu.

© 2022 Shemesh et al. This article is distributed under the terms of an Attribution–Noncommercial–Share Alike–No Mirror Sites license for the first six months after the publication date (see http://www.rupress.org/terms/). After six months it is available under a Creative Commons License (Attribution–Noncommercial–Share Alike 4.0 International license, as described at https://creativecommons.org/licenses/by-nc-sa/4.0/).

Downloaded from http://rupress.org/jem/article-pdf/219/11/e20220551/1441760/jem_20220551.pdf by guest on 28 September 2023

relapse (Zaghi et al., 2021; Merino et al., 2021), while in COVID-19 infection patients with poor outcomes display an adaptive NK cell expansion (Varchetta et al., 2021).

NK cell proliferation or expansion is regulated by IL-2, IL-15, and IL-12 (Wang and Zhao, 2021; Wiedemann et al., 2020; Shemesh et al., 2022), by the phosphorylation of STAT5 (pSTAT5), STAT4 (pSTAT4), and other STATs directly or indirectly, and by the activation of mammalian target of rapamycin (mTOR) complexes (Marçais et al., 2014; Anton et al., 2015; Anton et al., 2020). Activation of the mTOR complex-1 (mTORC1) leads to ribosomal protein S6 phosphorylation at position S235/236 (pS6S235/236) and regulates cap-dependent protein translation and cell cycle progression (Marçais et al., 2014). The mTOR complex-2 (mTORC2) phosphorylates AKT at position S473 (pAKTS473), which inhibits FOXO1 activity, a suppressor of cell cycle progression (Wang et al., 2018; Calnan and Brunet, 2008). TGFβ or IFNα can diminish NK cell proliferation by various signaling pathways with or without inhibition of mTOR activity (Platanias, 2005; Viel et al., 2016; Gartel and Tyner, 2002; Shemesh et al., 2022).

Here, we found a mechanism limiting FcRγ protein upregulation caused by diminished NK cell proliferation. Rapamycin treatment of lung transplant patients, low mTOR activity, and incubation of NK cells in the presence of rapamycin, TGFβ, or IFNα were, respectively, associated with lower FcRγ expression and an adaptive NK cell phenotype in healthy donors. Low FcRγ expression highly correlated with diminished cell proliferation. Additionally, we showed that during COVID-19 infection, NK cells with an adaptive-like phenotype increase in association with higher TGFβ and IFNα and disease severity. Our results suggest that alteration in signaling pathways leading to diminished NK cell proliferation support an adaptive-like NK cell phenotype. Further, in COVID-19 infection, early accumulation of adaptive-like NK cells can serve as an early prognostic biomarker associated with increased inflammation.

Results

Rapamycin treatment is associated with reduced FcRγ levels in NK cells from lung transplant patients

mTOR activity influences NK cell differentiation (Marçais et al., 2014; Yang et al., 2018). Rapamycin is an immune-suppressive agent used during solid organ transplantation with known mTOR selectivity (Sarbassov et al., 2006; Augustine et al., 2007; Calabrese et al., 2021). Therefore, we investigated if rapamycin treatment can alter the frequency of human NK cell subsets by comparing matched peripheral blood mononuclear cell (PBMC) samples obtained from lung transplant patients before and during rapamycin treatment (Fig. 1 A and Fig. S1 A). As a control comparison, we analyzed samples from lung transplant patients at least 1 yr after transplant while on standard immunosuppression but not rapamycin and matched for transplant indication. Using flow cytometry analysis, PBMCs were gated on live $CD45^+dump^-$ ($CD3^-CD19^-CD14^-CD123^-CD4^-$) $NKp46^+$, $CD56^+$ lymphocytes to identify NK cells, and then subgated the NK cells into four subsets based on NKG2A and CD16 expression: immature $NKG2A^+CD16^-$, immature $NKG2A^+CD16^{low}$, mature $NKG2A^+CD16^+$, and mature $NKG2A^-CD16^+$ (Fig. S1 B). Additionally, we examined markers associated with NK cell differentiation (CD57, NKG2C, and FcRγ), proliferation (Ki-67), and mTORC1 activity ($pS6^{S235/235}$). The percentage of NK cells within the $CD45^+$ population significantly increased during rapamycin treatment, possibly due to reduced T cell frequencies (Fig. S1 B). NK cell subset analysis showed a significant increase in mature $NKG2A^-CD16^+$ $CD57^+$ cells (Fig. 1 B). NKG2C expression did not correlate with FcRγ expression levels (Fig. S1 C). All the defined NK cell subsets displayed significantly lower FcRγ levels during rapamycin treatment (Fig.1 C and Fig. S1 D), accompanied by a lower percentage of $Ki\text{-}67^+$ cells and relatively fewer $pS6^{S235/236+}$ cells (Fig. 1, D and E). Overall, the results show that rapamycin treatment is associated with reduced mTOR activity, decreased cell proliferation, and lower FcRγ expression in human NK cells.

FcRγ expression at steady state is associated with mTOR activity

In healthy donors (HDs), reduced FcRγ expression is reported in immature and mature adaptive NK cells compared with FcRγ levels in mature nonadaptive NK cells (Hart et al., 2019). To evaluate if reduced mTOR activity is associated with lower FcRγ expression, we analyzed FcRγ expression and mTORC1/C2 activity in steady-state (resting) NK cells by flow cytometry. Additionally, we examined IL-2 receptor chain expression and downstream STATs and PI3K signaling as IL-2 signaling can influence FcRγ expression and mTORC1/C2 activity (Pahl et al., 2018; Wang and Zhao, 2021).

NK cells were isolated by negative selection from peripheral blood to avoid inadvertent stimulation during cell processing (Fig. 2 A). HDs were grouped into adaptive NK cell–positive HDs (positive for mature $NKG2A^-NKG2C^{high}FcR\gamma^-$ or $FcR\gamma^{low}$ NK cells, $n = 4$, all HCMV seropositive) or adaptive NK cell–negative HDs (negative for mature $NKG2A^{\pm}NKG2C^{\pm}FcR\gamma^{-/low}$ NK cells [Liu et al., 2016], $n = 9$ [3 HCMV-seropositive, 6 HCMV-seronegative]; Fig. 2 A; and Fig. S2, A and B). In all HDs, immature $CD56^{bright}CD16^-$ NK cells expressed low FcRγ levels (Fig. S2 A; Hart et al., 2019). Adaptive NK cell–positive HDs exhibited higher percentages of mature $NKG2A^-CD57^+$ cells, associated with NK cell maturation, relative to adaptive NK cell–negative HDs (Fig. S2 D; Björkström et al., 2010). Adaptive NK cells displayed reduced PLZF, Syk, CD161, Siglec-7, NKp30, and NKp46, while immature NK cells displayed a differential expression pattern with high levels of Syk, NKp30, NKp46, and CD25 (Fig. S3, A and B; Schlums et al., 2015; Lee et al., 2015).

Therefore, in adaptive NK cell–positive HDs, we compared cell signaling markers between immature $CD56^{bright}CD16^-$ and mature $CD56^{dim}CD16^+$ NK cells, further gated into the following subsets: nonadaptive $NKG2A^{-/+}NKG2C^-FcR\gamma^{high}$, adaptive $NKG2A^-NKG2C^{high}FcR\gamma^{low}$, and adaptive $NKG2A^-NKG2C^{high}FcR\gamma^-$, and between $CD57^-$ and $CD57^+$ cells within each of the defined mature subsets (Fig. 2 B). As a control, in adaptive NK cell–negative HDs, we examined the expression of signaling markers associated with NK cell maturation in the defined subsets: $NKG2A^+CD57^-$, $NKG2A^+CD57^+$, $NKG2A^-CD57^-$, and $NKG2A^-CD57^+$ (most mature; Fig. S2 D) to differentiate between

Downloaded from http://rupress.org/jem/article-pdf/219/11/e20220551/1441760/jem_20220551.pdf by guest on 28 September 2023

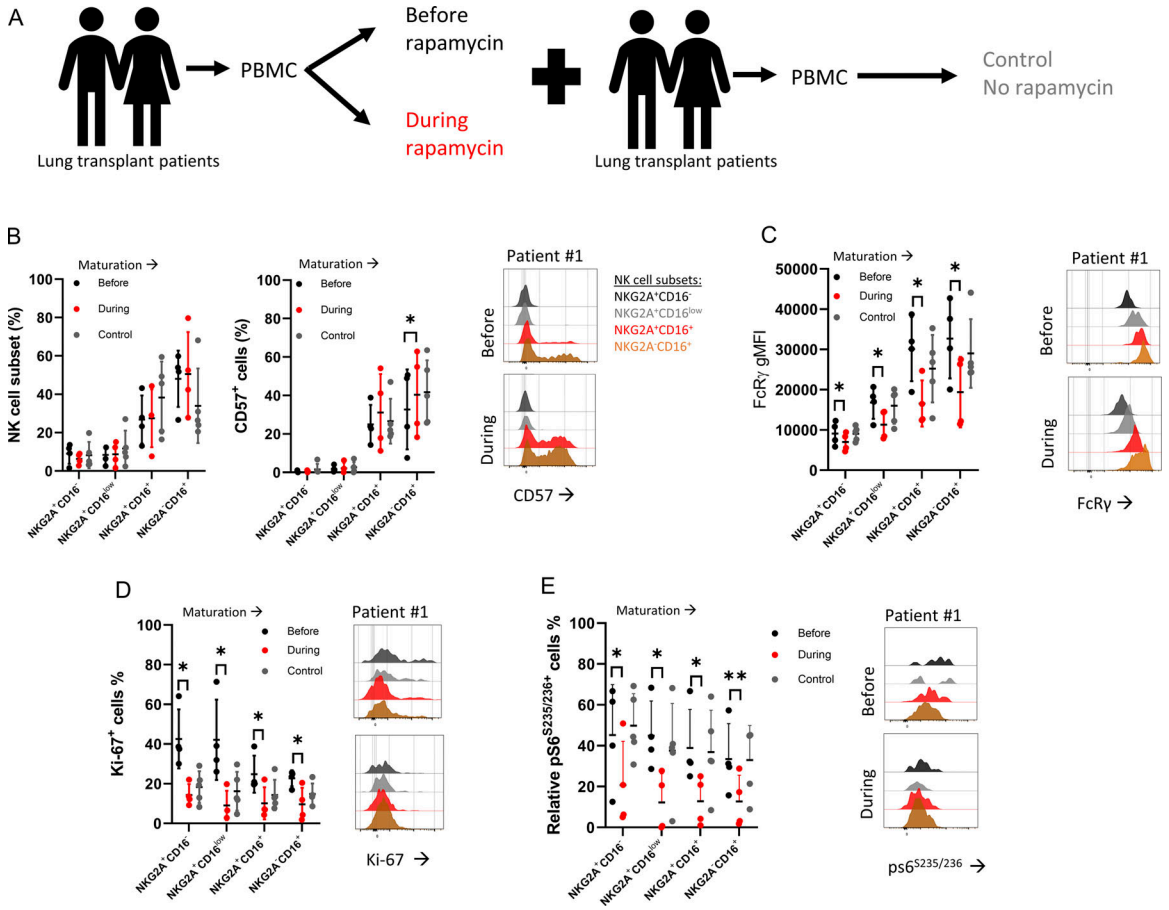

Figure 1. **FcRγ levels in NK cells from lung transplant patients during rapamycin treatment. (A)** Schematic of sample evaluation. PBMC samples from lung transplant recipients before or during rapamycin administration (n = 4) were assessed for NK cell subsets. Control group = patients at least 1-yr post-transplant and matched for transplant indication (n = 5). **(B)** Percentages of defined NK cell subsets and percentages of CD57$^+$ cells. Right: Representative histograms of CD57 staining in the defined NK cell subsets (color-coded; NKG2A$^+$CD16$^-$ [black], NKG2A$^+$CD16^{low} [gray], NKG2A$^+$CD16$^+$ [red], NKG2A$^-$CD16$^+$ [orange]) before and during rapamycin treatment. **(C)** FcRγ gMFI in the defined NK cell subsets, with representative histograms before and during rapamycin treatment in the defined NK cell subsets (color-coded). **(D)** Percentages of Ki-67$^+$ NK cells in the defined NK cell subsets, with representative histograms before and during rapamycin treatment in the defined NK cell subsets (color-coded). **(E)** Relative pS6$^+$ NK cells in the defined NK cell subsets, with representative histograms before and during rapamycin treatment in the defined NK cell subsets (color-coded). Statistical analysis was done between matched samples, mean ± SD, paired t test, parametric. *, P ≤ 0.05; **, P < 0.01.

adaptive-associated or maturation-associated cell signaling alterations (Björkström et al., 2010).

STATs phosphorylation, examined by pSTAT1^{Y701}, pSTAT4^{Y693}, or pSTAT5^{Y694} expression levels (Wiedemann et al., 2021), were lower in the adaptive FcRγ$^-$ or FcRγ^{low} subsets relative to nonadaptive mature NKG2C$^-$FcRγ^{high}CD57$^-$ NK cells (normalization index = 1), and increased in immature CD56^{bright}CD16$^-$FcRγ^{low} NK cells (Fig. 2 B and Fig. S3 B). In line with the lower STATs activity, CD122 expression decreased with the adaptive phenotype (Fig. 2 C). In HDs without adaptive NK cells STATs activity and CD122 expression were reduced with NK cell maturation relative to immature NK cells (Fig. 2, D and E). However, mature CD57$^+$ cells exhibited increased STATs activity relative to mature CD57$^-$ cells (Fig. 2 D) and further reduced CD122 levels. Yet these changes did not translate to changes in FcRγ levels (Fig. 2, E and F; Björkström et al., 2010). Therefore, we concluded that the reduced FcRγ expression is not directly associated with reduced STATs activity or reduced CD122 expression in peripheral blood adaptive NK cells.

PI3K activity (pAKT^{T308}; Mace, 2018) showed no significant differences between the defined adaptive NK cell subsets (Fig. 3 A and Fig. S3 B). However, mTOR activity measured by pS6$^{S235/236}$ (mTORC1) or pAKT^{S473} (mTORC2; Wang and Zhao, 2021; Yang et al., 2015) was significantly lower in immature CD56^{bright}CD16$^-$ NK cells and adaptive FcRγ^{low} or FcRγ$^-$ NK cell subsets. Moreover, we detected reduced mTOR protein levels while Bcl2 expression was high in adaptive NK cells (Fig. 3 A; Barnes et al., 2020). In adaptive NK cell–negative donors, PI3K activity decreased with cell maturation (Fig. 3 B). mTOR activity (specifically mTORC2 [pAKT^{S473}]) was lower in immature NK cells with no difference in mature NK cell subsets (Fig. 3 B). mTOR protein decreased with maturation, and Bcl2 expression increased (Fig. 3 B). These results indicated that the FcRγ$^{-/low}$ phenotype, observed in peripheral blood immature NK cells and

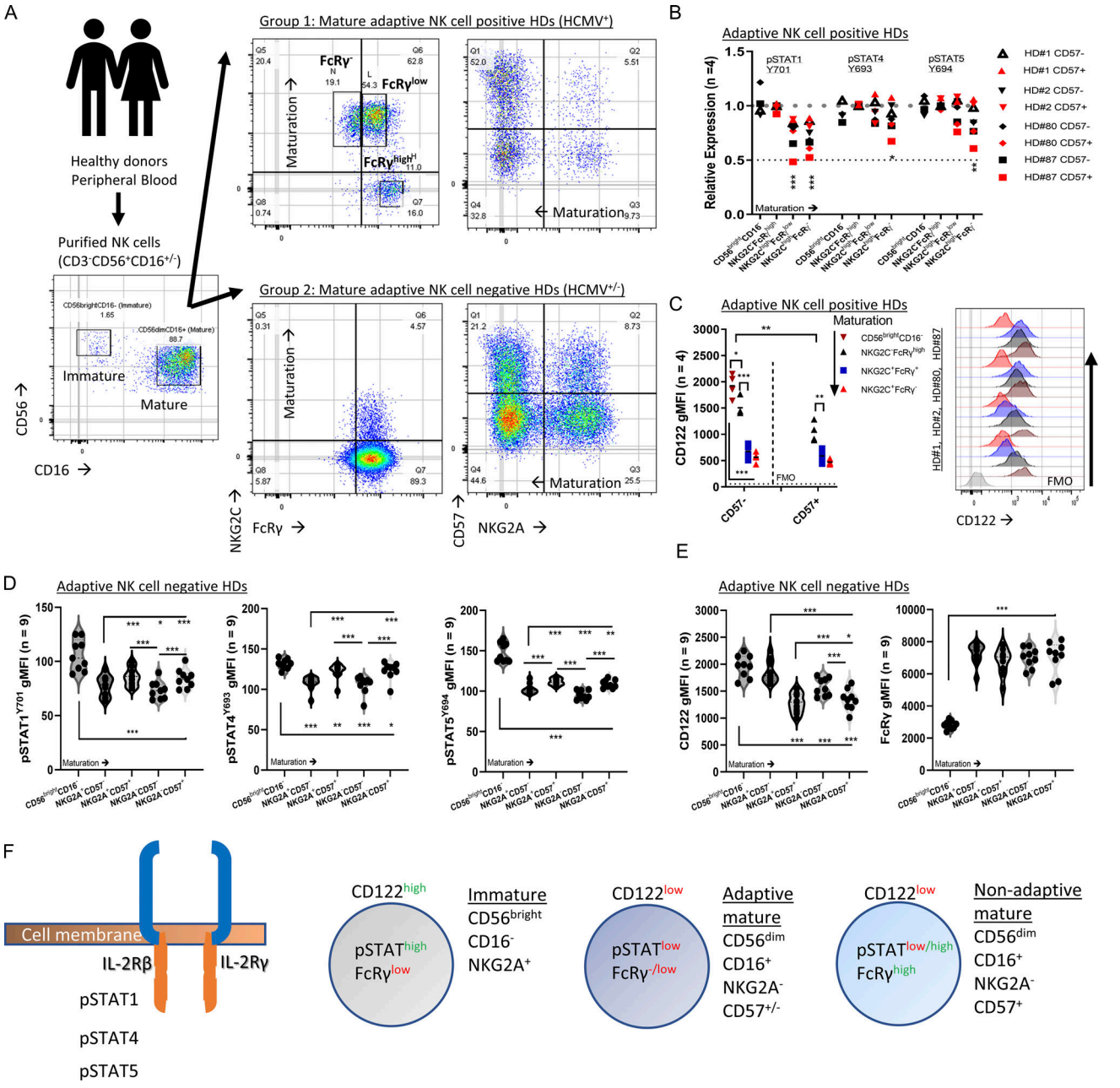

Figure 2. **FcRγ expression at steady state is associated with mTOR activity.** Purified primary NK cells were examined ex vivo, without additional stimulation, for the indicated markers. *n* = number of donors, paired *t* test, parametric. *, P < 0.05; **, P < 0.01; ***, P < 0.001. **(A)** Peripheral blood samples were obtained from healthy donors. NK cells (CD3⁻CD56⁺CD16±) were purified by negative selection from peripheral blood samples and classified into Group 1 (adaptive NK cell–positive HDs [#1, 2, 80, 87; HCMV-seropositive]) and Group 2 (adaptive NK cell–negative HDs [#77, 82, 86, 88, 89, 91, HCMV-seronegative; and 78, 84,85, HCMV-seropositive]). Gating strategy: CD3⁻CD56⁺CD16± NK cells were gated as immature $CD56^{bright}CD16^{-}$ and mature $CD56^{dim}CD16^{+}$. In adaptive NK cell–positive HDs, mature NK cells were examined for NKG2C and FcRγ expression and gated as $NKG2C^{high}FcR\gamma^{negative}$, $NKG2C^{high}FcR\gamma^{low}$, and $NKG2A^{\pm}NKG2C^{negative}FcR\gamma^{high}$ NK cells. For NK cell maturation, NK cells were gated as NKG2A versus CD57. **(B)** Relative expression of phospho-$STAT1^{Y701}$, $STAT4^{Y693}$, and $STAT5^{Y694}$ in the indicated NK cell subsets in adaptive NK cell–positive HDs from 4 HDs. The gMFI values were determined for the indicated NK cell subsets and were then normalized relative to the gMFI values measured for the mature nonadaptive $NKG2C^{-}FcR\gamma^{high}CD57^{-}$ NK cells in the same donor, which were established as index = 1 (upper dashed line), index = 0.5 (lower dashed line). **(C)** Expression of CD122 in the indicated NK cell subsets in adaptive NK cell–positive HDs. Right: Histograms of CD122 expression per NK cell subset for each donor (color-coded; horizontal dashed line = FMO control values). **(D)** Expression of $pSTAT1^{Y701}$, $pSTAT4^{Y693}$, and $pSTAT5^{Y694}$ in the indicated NK cell subsets in adaptive NK cell–negative HDs. Violin plots. **(E)** Expression of CD122 and FcRγ in the indicated NK cell subsets in adaptive NK cell–negative HDs. Violin plots. **(F)** Schematic of examined signaling and associated markers in the defined NK cells subsets.

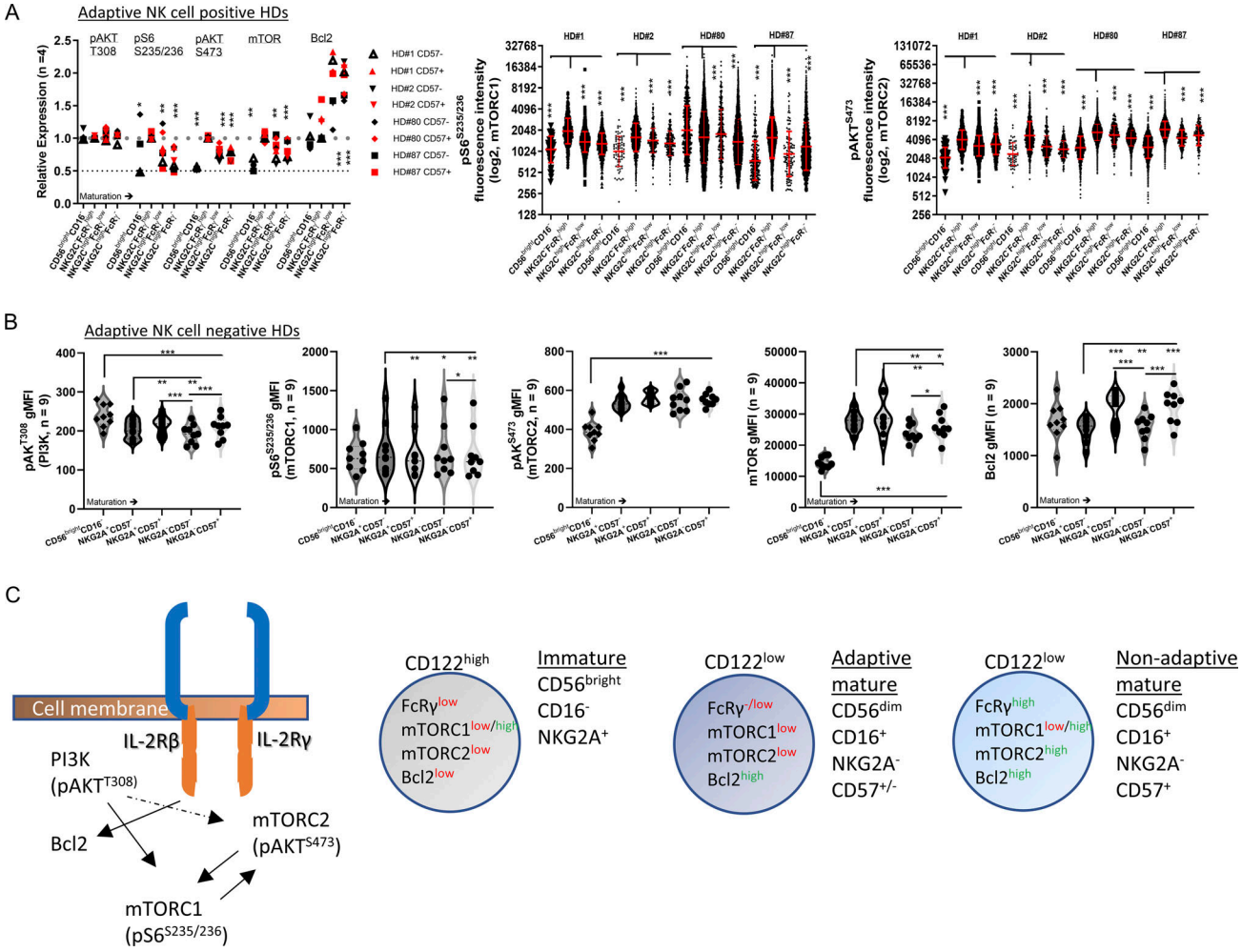

Figure 3. **PI3K and mTOR activity in immature, mature, and adaptive NK cells. (A)** Relative expression of pAKT^{T308} (PI3K activity), pS6$^{S235/236}$ (mTORC1), pAKT^{S473}(mTORC2), mTOR protein, and Bcl2 protein in the indicated NK cell subsets in adaptive NK cell–positive HDs. Expression was normalized relative to NKG2C$^-$FcRγ^{high}CD57$^-$ cells that are index = 1 (upper dashed line), index = 0.5 (lower dashed line). Paired *t* test. *, P < 0.05; **, P < 0.01; ***, P < 0.001. Right: Single-cell expression of (left to right) pS6$^{S235/236}$ or pAKT^{S473} (log_2 values). Red bar = geometric mean ± SD unpaired *t* test, two tails. *, P < 0.05; ***, P < 0.001. **(B)** Expression of (left to right) pAKT^{T308} (PI3K), pS6$^{S235/236}$ (mTORC1), pAKT^{S473}(mTORC2), mTOR protein, and Bcl2 protein in the indicated NK cell subsets in adaptive NK cell–negative HDs. Violin plots, paired *t* test, parametric. *, P < 0.05; **, P < 0.01; ***, P < 0.001. **(C)** Schematic of the examined signaling and associated markers in the defined NK cells subsets.

mature adaptive NK cells, is associated with reduced mTOR activity (Fig. 3 C).

Peripheral blood FcRγ$^{-/low}$ NK cells exhibit a differential FOXO1–EOMES–T-bet phenotype

mTORC2 suppresses the activity of the transcription factor FOXO1, a positive regulator of the transcription factor EOMES and a negative regulator of the transcription factor T-bet (Deng et al., 2015; Gordon et al., 2012). Both EOMES and T-bet regulate CD122 expression (Zhang et al., 2018). Therefore, we investigated FOXO1 activity in immature, mature nonadaptive, and adaptive NK cell subsets by examining T-bet, EOMES, and FOXO1 protein expression. T-bet levels were significantly lower in immature CD56^{bright}CD16$^-$ and adaptive FcRγ^{low} or FcRγ$^-$ NK cells relative to mature nonadaptive NK cells and similar to mTORC2 activity (Fig. 4 A). Accordingly, immature NK cells expressed higher EOMES and FOXO1 levels, explaining the higher expression of CD122. However, adaptive NK cells expressed low EOMES and FOXO1 levels, explaining the decrease in CD122 expression (Fig. 4 A). In adaptive NK cell–negative HDs, T-bet levels increased with NK cell maturation, demonstrating a different expression pattern relative to adaptive NK cells (Fig. 4 B; Björkström et al., 2010). However, and in line with the reduced CD122 levels, EOMES and FOXO1 expression decreased with NK cell maturation, indicating that the reduction of these proteins is not specifically associated with the adaptive NK cell phenotype (Fig. 4 C). The results suggest a differential signaling regulation associated with alteration in mTORC2–FOXO1 activity and reduced FcRγ expression (Figs. 3 C and 4 C), whereas immature FcRγ^{low} NK cells are CD122^{high}, mTORC2^{low}, FOXO1^{high}, EOMES^{high}, and T-bet^{low}, and adaptive FcRγ^{low} or FcRγ$^-$ NK cells are CD122^{low} mTORC2^{low}, FOXO1^{low}, EOMES^{low}, and T-bet^{low}. Mature nonadaptive NKG2A$^-$CD57$^+$ NK cells, which are FcRγ^{high}, exhibited a CD122^{low}, mTORC2^{high}, FOXO1^{low}, EOMES^{low}, and

Downloaded from http://rupress.org/jem/article-pdf/219/11/e20220551/1441760/jem_20220551.pdf by guest on 28 September 2023

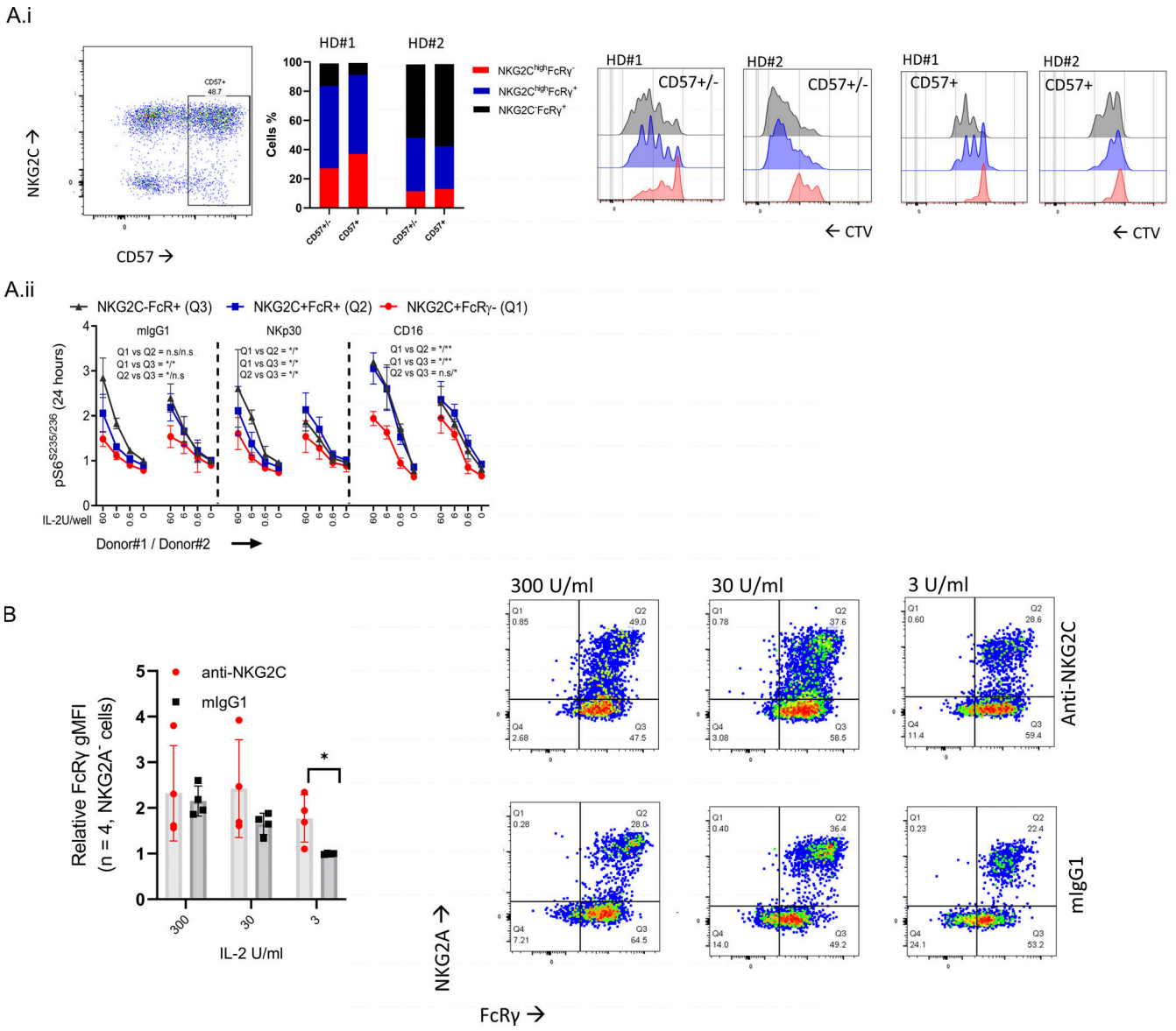

Figure S5. **Influence of CD16 or NKG2C stimulation on adoptive FcRγ$^{-/low}$ NK cells. (A i)** NK cell proliferation (CTV assay) of sorted CD57^{+} vs. unsorted CD57$^{\pm}$ adaptive vs. nonadaptive NK cells from HDs #1, #2 after stimulation with anti-CD16 + IL-2 (6 U/ml). **(A ii)** Normalized pS6 gMFI levels after 24 h of the indicate stimulation in the defined mature NK cell subsets. Mean ± SD. Paired *t* test, two tails, *, P < 0.05; **, P < 0.01. **(B)** FcRγ levels of NKG2A^{-} NK cells in donors with adoptive NK cells (Fig. S2). Cells were stimulated with anti-NKG2C-coated or mouse IgG1 isotype-matched control-coated beads for 6 d in the presence of increasing IL-2 concentrations. Mean ± SD. Paired *t* test, parametric. *, P < 0.05.

Downloaded from http://rupress.org/jem/article-pdf/219/11/e20220551/1441760/jem_20220551.pdf by guest on 28 September 2023